Swell Waves Monitored by HF Ocean Surface Radar at Tweed Heads and Bass Strait

Jonathan S. Bathgate and Mal Heron

School of Mathematical and Physical Sciences, James Cook University, Townsville 4811, AUSTRALIA

Abstract

HF ocean surface radar is routinely used to measure surface currents and wind wave parameters over large areas of the ocean surface. The new algorithm presented here provides a fast method of extracting swell wave parameters using frequency modulation theory and is an improvement on existing wave spectrum analyses for routine swell detection. Swell parameters are produced from second-order (sideband) energy about the first-order Bragg peaks in the spectrum. The algorithm utilizes the relationship between these sidebands and the first-order to derive swell parameters including direction, height and period. The data used to develop this algorithm were collected at two sites during 2001 using COSRAD (Coastal Ocean Surface Radar). The first deployment of this study occurred during February and March, 2001, at Tweed Heads. The second deployment occurred during July, 2001, monitoring the seaward side of the entrance to Port Phillip Bay. The radar was configured here to aid in the extraction of swell wave parameters. Both locations were selected so that radar coverage would overlap directional wave buoys operated by QBPA and Port of Melbourne Corporation. These wave buoys provided validation sets for the measured swell wave parameters and the results indicate that the COSRAD HF radar is suitable for monitoring swell in the near-shore zone.

1 Introduction

HF radar has been widely used in recent years for mapping surface currents and wind waves over large areas of the ocean surface. This kind of monitoring aids in a diverse range of fields such as coastal management, biological research and environmental monitoring. It also has applications in some locations as a coastal safety/security system for the prevention of illegal activity in the coastal zone and as an aid to coast guards on occasions of shipping accidents (Sevgi *et al.*, 2001). The use of HF radar in the context of this article lies in the monitoring of long ocean waves or swell waves. Since Crombie (1955) mathematically described the relationship between HF radar transmissions and the sea surface, direct measurement of the relatively short surface waves (Bragg waves) that are used to detect surface currents has become common. Surface current direction and velocity can be mapped at high resolutions and accuracies. The technique has been validated on numerous occasions by directional wave buoys (Prytz et al. 1999; Heron et al. 2001) and is now a routine procedure.

However, advancements in the measurement of longer ocean waves such as swell have been slow. At HF, information on this portion of the ocean wave spectrum is a second-order effect. This part of the spectrum is far more complicated and susceptible to noise than the first-order spectrum that yields surface current information (Figure 1). Mathematical solutions for the extraction of swell wave parameters have been understood for some time (Barrick, 1972b; Lipa et al. 1980) however routine measurement of these waves still proves elusive. The sensitivity of these solutions requires a high level of data quality that is seldom available in the second-order portion of the Doppler spectrum.

A coastal ocean surface radar system (COSRAD) that was developed at James Cook University was employed to collect data for the development of a new method for the extraction of swell height, direction and period.

Some results from this new method will be presented here to show the ability of the algorithm to simultaneously monitor swell, surface currents and wind waves.

2 COSRAD Deployments

Two deployments of the COSRAD system occurred in 2001. Each deployment was of one month duration. Firstly, at Tweed Heads in February and March and then at the entrance to Port Phillip Bay in Victoria monitoring waters in Bass Strait during July. Both deployments were supported by directional wave buoys that provided a validation data set in the coverage zone. Figures 2 and 3 show
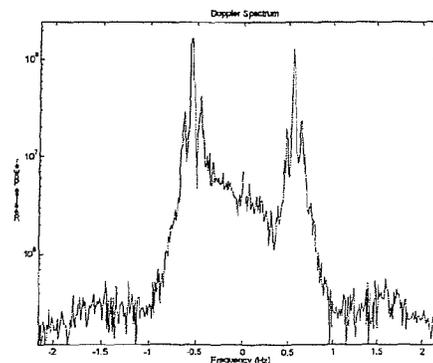

Figure 1 Portion of an averaged Doppler spectrum showing the two prominent first-order lines and the surrounding second-order lines.

these deployments at Tweed Heads and Bass Strait respectively.

The location and time of year were chosen in the case of Tweed Heads to coincide with the implementation of a sand by-pass system at the Tweed River entrance (Dyson et al. 2001). The primary interest here was the mapping of surface currents and possible impact they may have on the new by-pass system. This was, however, a good data set for the development of a new algorithm for swell parameter extraction. The Bass Strait deployment was chosen specifically for the likelihood of encountering strong swell conditions during the deployment.

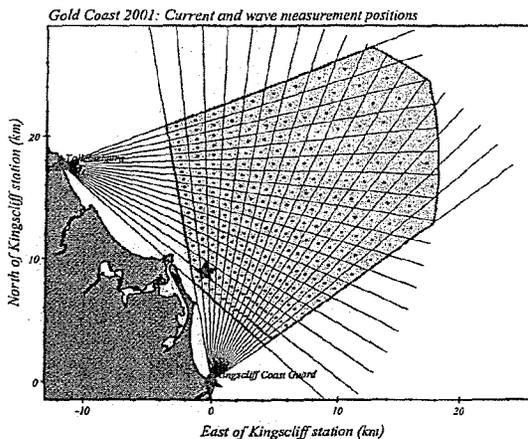*Gold Coast 2001: Current and wave measurement positions*

Figure 2 Coverage area of the deployed COSRAD system at Tweed Heads. The triangles represent the two radars and the star is the directional wave buoy operated by the Queensland Beach Protection Authority (QBPA).

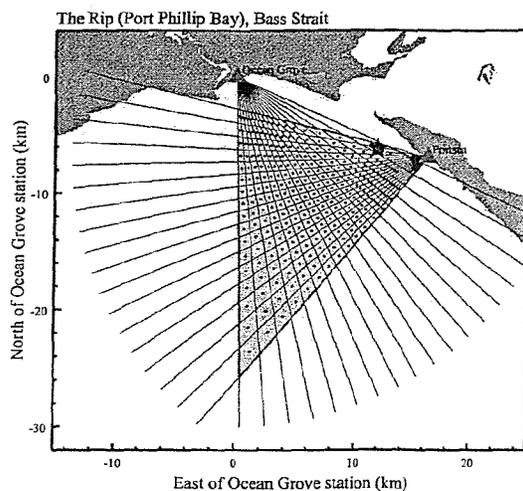The Rip (Port Phillip Bay), Bass Strait

Figure 3 Coverage area of the COSRAD system monitoring the entrance to Port Phillip Bay. The directional wave buoy here is maintained by the Port of Melbourne Corporation.

2.1 COSRAD Configuration

The COSRAD system transmits at a frequency of 30 MHz which gives the radar wave a length of 10 m. It is a phased array system with a common transmit/receive array. The antenna array consists of 8 elements spaced half a transmit wavelength apart and therefore spans a total 45 m. The array forms a beam that is 7 degrees in width and is steered electronically to 17 different angles. Each of these angles forms a sector and the backscattered radar wave is monitored at 12 ranges in each sector. The range resolution is set at 3 km. Therefore, each radar covers a sweep of approximately 60 degrees. The time taken to collect data at each range can be varied depending upon the interests of the deployment. At Tweed Heads the dwell time at each point was such that an entire sweep was completed every 30 minutes. This allowed a greater temporal resolution for examining highly variable surface current activity. At Bass Strait this dwell time was doubled so that an entire sweep took 60 minutes to complete. The objective of this deployment was to measure swell which is less susceptible to variations in local conditions. This increased dwell time increased the resolution of the Doppler spectrum to aid in the identification of the second-order features that contain the swell information.

2.2 Spectral Pre-Processing

In order to extract information from the second-order echo the peaks must be routinely identifiable in the spectrum. These peaks are often subject to interference from the surrounding noise floor resulting in bifurcations and broadening. To minimize these effects and maximise the correct identification of these peaks several individual spectra are averaged spatially and temporally. Due to the nature of swell, we found it is acceptable to average the data over a 2 hr period without noticeable loss of information. We also average spatially over a total 8 range cells, 4 cells in 2 adjacent sectors. This improves the signal to noise ratio in the second-order spectrum which is vital to the extraction of information from the swell peaks. Peak normalization is also employed to remove the effects of signal attenuation at long range. The Doppler shift due to surface currents is also removed prior to the incoherent averaging process.

3 Frequency Modulation Model

This new method of swell wave measurement relies on a modulation in frequency imposed upon the short Bragg waves by the longer, faster moving, swell. As the swell passes through it imparts a surge velocity on the shorter Bragg waves as shown in Figure 4. The Bragg waves are thrust forward at the crests and backward at the trough. This surge velocity is calculated as,

$$v_S = a_S \omega_S \qquad (1)$$

where a_s is the amplitude of the swell wave, and ω_s is the frequency, and the trajectory of the surface parcel is a circle in the vertical plane. The horizontal component of the surge velocity is

$$v_{SH} = a_S \omega_S \cos(\omega_S t) \qquad (2)$$

If we wish to consider the swell surge velocity in a direction θ from the direction of propagation of the swell, then it is a simple projection and the horizontal component is given by
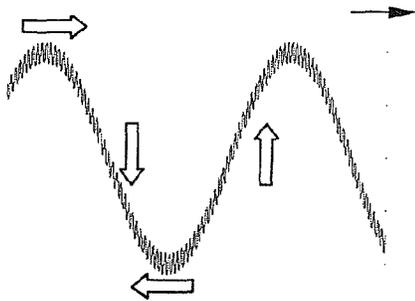
$$v_{SH} = a_S \omega_S \cos\theta \cos(\omega_S t) \qquad (3)$$

Figure 4 Schematic of a two-scale system with a short wavelength Bragg wave riding on a swell. The arrows show the instantaneous velocity of the surface water particles in response to the swell wave. The surge velocity of the swell wave modulates the instantaneous velocity of the Bragg wave and when the radar wave backscatters, the echo is frequency modulated.

We can therefore extract information on the swell by observing this relationship from various angles as the radar sweeps across its 60 degree range. We know that the Doppler spectrum will show the most energetic sidebands, strongest component of the modulation, when the radar is pointing in the direction of swell propagation and no sidebands when it is directed along the swell crests. To measure this relationship a parameter R_{swell} is extracted from the spectrum. R_{swell} is calculated as the ratio of the first-order Bragg amplitude to the mean amplitude of the first sidebands, as shown in Figure 5.

The R_{swell} value will be at its minimum when the radar beam is looking in the direction of swell propagation, when $\theta = 0$. A larger ratio will be found when the radar beam is at an angle to the direction of propagation due to the smaller component of the modulation being captured by the radar beam. When $\theta = 90$ the modulation seen in this direction is zero and thus the R_{swell} value
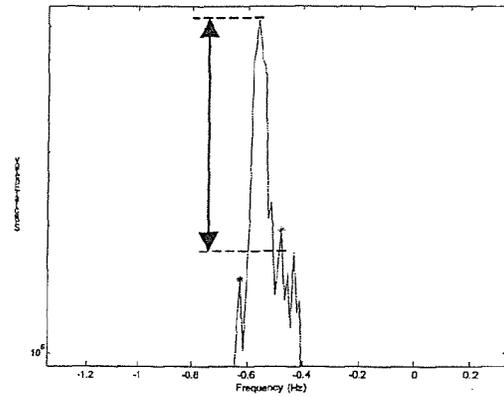

Figure 5 The receding first-order Bragg line with surrounding sidebands marked with asterisks. The dashed lines represent the amplitude of the Bragg line and the mean amplitude of the sidebands. The R_{swell} parameter is the ratio of these values.
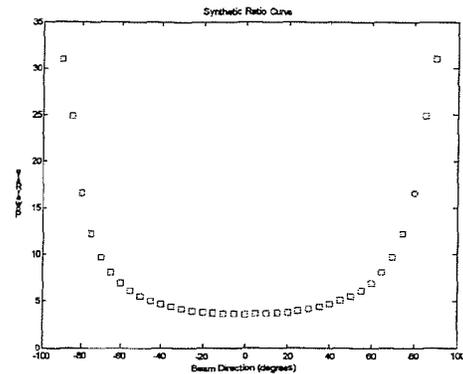

Figure 6 Synthetic curve of R_{swell} values calculated for beam directions 0 to 90 degrees at an arbitrary amplitude. A full curve is formed by reflecting about zero degrees.

approaches infinity. Figure 6 shows a synthetic curve of R_{swell} values that represents this relationship. The swell direction is arbitrarily given as zero degrees and thus the minimum of the curve is reflected about this value. When R_{swell} calculated from real data as in Figure 5 it can then be fitted to the synthetic curve in order find the swell direction by manipulating the curve in the X domain, and the height by fitting in the Y domain.

Swell period is calculated independently of the above method. It is simply the inverse of the mean frequency displacement of the Bragg line to the first sidebands. This is a very accurate and reliable method. If one or more sidebands are affected by noise then the remaining sidebands are used to provide a result.

4 Results

A day of swell parameters, height, direction and period, as measured by this new method at both Tweed Heads and Bass Strait are validated here by directional wave buoy data. The Tweed Heads data

193

was chosen as an example of strong swell conditions and the Bass Strait data was chosen to show the performance of the algorithm in lower swell conditions. The results below are measured by the Tallebudgera station at Tweed Heads and the Portsea station at Bass Strait. These stations were chosen due to the favourable angle they form with swell direction at these times. The bore sight of the Tallebudgera station is 99 degrees east of north which is close to the average swell direction of 100 degrees on March 5. The Portsea station forms a greater angle with the swell on July 18, propagating towards 190 degrees east of north but is still in a good position to observe the swell. The bore sight at Portsea is 252 degrees east of north

4.1   Tweed Heads, March 5, 2001

This day saw the largest swell waves encountered during both deployments reaching a maximum of just less than 1 m. Figure 6 shows good agreement between the wave buoy and the measured heights calculated using COSRAD data. The swell height is measured here with an rms error of only ±0.08 m. The measured swell direction (Figure 7) also compares well with the wave buoy. The COSRAD measurements agree with rms errors of ±10.5 degrees. Swell period is also accurately mapped to within ±0.75 second.
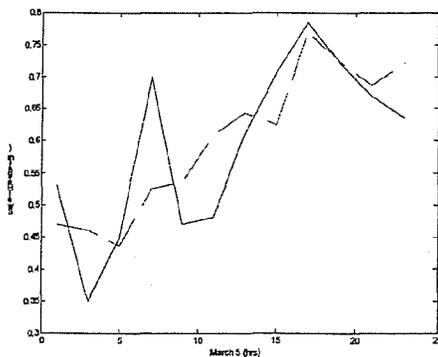

Figure 6 Comparison of swell height on March 5, 2001 at Tweed Heads as measured using COSRAD data (solid line) and the directional wave buoy (dashed line).
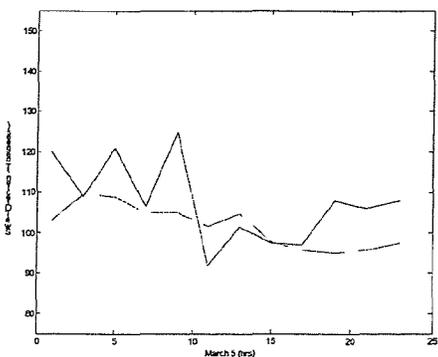

Figure 7 Comparison of swell direction on March 5, 2001 at Tweed Heads as measured using COSRAD

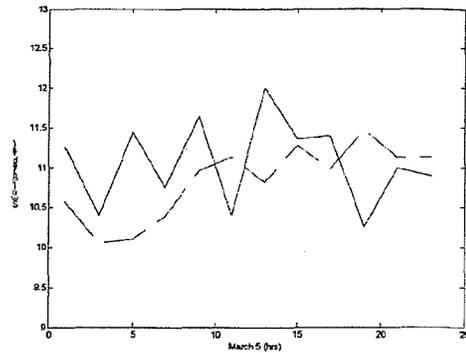data (solid line) and the directional wave buoy (dashed line).

Figure 8 Comparison of swell period on March 5, 2001 at Tweed Heads as measured using COSRAD data (solid line) and the directional wave buoy (dashed line).
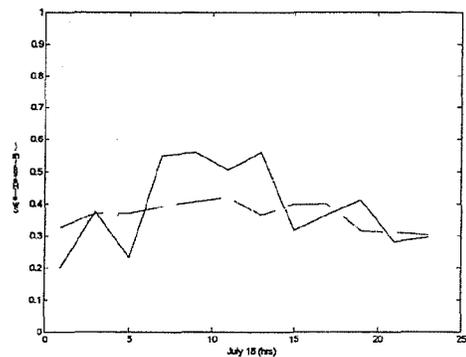

Figure 9 Comparison of swell height on July 18, 2001 at Bass Strait as measured using COSRAD data (solid line) and the directional wave buoy (dashed line).
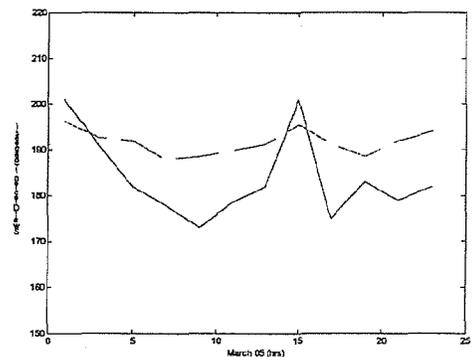

Figure 10 Comparison of swell direction on July 18, 2001 at Bass Strait as measured using COSRAD data (solid line) and the directional wave buoy (dashed line).

4.2   Bass Strait, July 18, 2001

Similar accuracies for each parameter were found in the analysis of data at Bass Strait even though the swell conditions were not as strong as those at Tweed Heads. The swell heights here reached a maximum of 0.42 m (Figure 9). The swell height

194

was still measured with an rms error of only ±0.11 m. Swell direction and period are still
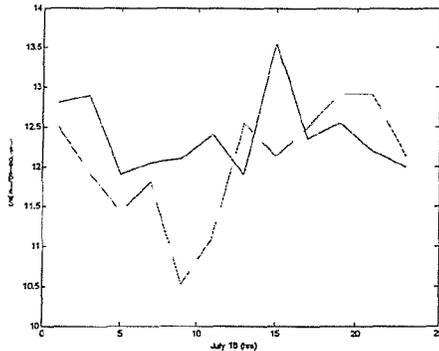

Figure 11 Comparison of swell period on July 18, 2001 at Bass Strait as measured using COSRAD data (solid line) and the directional wave buoy (dashed line).

measured with rms errors of ±10.45 degrees (Figure 10) and ±0.85 seconds (Figure 11) respectively. These results add confidence in the algorithm to perform in weak swell conditions. A small increase in error for swell height and period were found in the accuracies of the Bass Strait measurements when compared to those of the Tweed Heads study however this increase is very small and is expected at low swell heights.

5 Discussion

Monitoring long period ocean waves has previously been the responsibility of in situ instruments such as directional waverider buoys. This new method provides continuous real-time measurement of swell waves over significant areas of the coastal zone. This information could be used to influence decisions in many areas including coastal management and port safety. The impact of storm induced wave events on coastal regions can be severe and the monitoring of these waves can provide coastal engineers with valuable information for safeguarding coastal structures against such events (Ruggerio *et al.*, 1997).

The ability of this algorithm to function to the accuracies stated above with existing radar configurations while simultaneously extracting surface currents and wind wave parameters is a valuable attribute to ocean monitoring HF radar systems. The measurement of swell with this method is still possible even when the ocean surface is confused by a strong locally driven sea. The automated swell algorithm will remain unaffected by wind-waves of any amplitude so long as there is a separation between the peaks in the frequency spectrum. The swell algorithm depends on consistent and reliable identification of the swell peaks. However, under some circumstances this identification can become problematic. These situations include extremely weak, low amplitude, swell or bimodal swell. Weak swell conditions

result in poorly developed spectral peaks while bimodal swell produces bifurcations in the sidebands. Both situations reduce consistency in identification. In low amplitude swell conditions there is considerably less interest in swell measurement as it ceases to be a hazard to shipping and coastal communities. Bimodality usually occurs only for short periods when two separate swell sets are of similar amplitude but travelling in different directions. In the existing version of the algorithm only the dominant swell is measured. Resolving issues of bimodality will require additional attention in future revisions.

6 Conclusions

The results presented here support the fact that coastal ocean surface radar can be effectively employed to monitor long ocean waves, swell, in the near shore zone in a variety of conditions. This new method requires no changes to radar configuration and produces results alongside the extraction of surface currents and wind waves.

With this new capability the COSRAD HF radar is now able to monitor;
- Surface currents;
- Wind direction;
- Rms wave height and
- Swell period, direction and height.

New generation radar systems with beam forming capability are now producing these products in coastal water to ranges up to 200 km.

8 References

Barrick, D. E. 1972b: Remote sensing of sea state by radar. In *Remote Sensing of the Troposphere, ed. V. E. Derr* 12-1 to 12-46.

Crombie, D. D., (1955) Doppler spectrum of sea echo at 13.56Mc/s. *Nature, 175: 681-682.*

Dyson, A., Victory, S. and Connor, T. (2001) Sand Bypassing the Tweed River Entrance: An Overview. *Proceedings, 15th Australasian Coastal and Ocean Engineering Conference ('Coasts and Ports 2001'),* 310-315.

Heron, M. L, Prytz, A. and Bathgate, J. S. (2001) Currents off Tweed Heads by HF ocean surface radar, *Coastal and Ocean Eng. Conf., IEAust.*, 49-54.

Lipa. B, and Barrick, D. 1980. Methods for the extraction of long-period ocean wave parameters from narrow beam HF radar sea echo, *Radio Science*, 15: 843-853.

Prytz, A. and Heron, M. L. (1999). On the flushing of Port Phillip Bay: an application of HF ocean radar, *Mar. Freshwater Res.*, 50: 483-492.

Ruggiero, P., Kaminsky, G. M., Komar, P. D. and W. G. McDougal, 1997. Extreme waves and coastal erosion in the Pacific Northwest. *Ocean Wave Measurement and Analysis, Proceedings of the 3rd International Symposium, Waves '97*, 947-961.

Sevgi, L., A. Ponsford, and H. C. Chan, 2001: An integrated maritime surveillance system based on High-Frequency surface-wave radars, Part 1: Theoretical background and numerical simulations. *IEEE Antennas and Propagation Magazine*, **43**, 28-43.